UNIVERSITY OF CALIFORNIA SAN DIEGO

The Role of Calcium Dependent Protein Kinase 32 in the Triggered Immune Responses of *Arabidopsis thaliana*

A Thesis submitted in partial satisfaction of the
requirements for the degree Master of Science

in

Biology

by

Ruonan Wang

Committee in charge:

Professor Alisa Huffaker, Chair
Professor Steve Briggs
Professor Yunde Zhao

2018

The Thesis of Ruonan Wang is
approved, and it is acceptable in quality and form for publication on
microfilm and electronically:

_____

_____

_____
Chair

University of California San Diego

2018

DEDICATION

Foremost, this is dedicated to my loving mom, Min Zhou. You are an incredible woman, always providing encouragement, support, and love. Through the busiest and hardest of times, you remain filled with spirit and optimism. Your humors are always the best.

I would also like to dedicate this to my amazing dad, Lansheng Wang.
You are a strong man, always giving decent suggestions and encouragement, teaching me how to study, work and live. I would not complete my life goals without your support.

EPIGRAPH

“One must still have chaos in oneself to be able to give birth to a dancing star.”

Friedrich Nietzsche

TABLE OF CONTENTS

LIST OF FIGURES

LIST OF TABLES

LIST OF SUPPLEMENTAL FIGURES

Acknowledgments

I would like to thank Dr. Alisa Huffaker for her support as my advisor and as the committee chair. Whether in the laboratory or other fields of life, her enthusiasm provides a source of inspiration for me. I am thankful for all of her advice and guidance. Furthermore, I am grateful for her persistence and patience throughout the many edits of this thesis dissertation script.

I would like to thank Dr. Steve Briggs and Dr. Yunde Zhao for being members of my committee.

I would also like to thank Dr. Steve Briggs and Dr. Zhouxin Shen for providing the phosphoproteomic analysis data.

Certainly, this thesis would not have been possible without Dr. Philipp Weckwerth and Dr. Keini Dressano. Thanks to Dr. Philipp Weckwerth for providing the mutual rank analysis data and CPK32-YFP transient expression images. Thanks to Dr. Keini Dressano for providing the yeast-two-hybrid protein interaction figures. Special thanks to Dr. Philipp Weckwerth for being my mentor in my lab training and guiding me in various experiments. Special thanks to Dr. Keini Dressano for providing me many protocols for essential experiments. I am grateful for their patience throughout the many edits of this thesis dissertation. Special thanks to Mr. Elly Poretsky for providing the amazing mutRank program for the lab in general.

Last but not least, I would like to thank all the members of Huffaker lab for their guidance and moral support.

ABSTRACT OF THE THESIS

The Role of Calcium Dependent Protein Kinase 32 in the Triggered Immune Responses of *Arabidopsis thaliana*

by

Ruonan Wang

Master of Science in Biology

University of California San Diego, 2018

Professor Alisa Huffaker, Chair

Arabidopsis thaliana Plant Elicitor Peptide 1 (AtPep1) is an endogenous peptide that interacts with its membrane embedded receptors PEPR1 and PEPR2 to amplify Damage- and Pathogen-associated molecular pattern (DAMP and PAMP)-triggered immunity (Huffaker *et al.,*

2006; Ross *et al.*, 2014). The Huffaker lab identified putative novel components regulating innate immune responses in *Arabidopsis* by examining the alterations in phosphorylation states of proteins after peptide treatment. In this study of AtPep1-triggered immunity, one of the identified candidates, calcium-dependent protein kinase 32 (CPK32), has been characterized. From previous studies and preliminary data, the structure and localization of CPK32 have been roughly established. However, the function of CPK32 in DAMP and PAMP-triggered immune responses has not been identified. In this thesis report, it was investigated how CPK32 affected Pep-induced plant defense and growth in *Arabidopsis*. This study focuses on characterizing early signaling events in the *cpk32* knockout mutants, *cpk32-1* and *cpk32-2*, including rapid burst of reactive oxygen species (ROS), activation of mitogen activated protein kinase (MAPK), and defense gene expression changes. To address the biological relevance and elucidate the function of CPK32 in plant resistance to bacteria and fungus, *cpk32* mutants were infected with biotrophic and necrotrophic pathogens, *Pseudomona syringae* pv tomato DC30000 (*Pst* DC3000) and *Botrytis cinerea* (*B. cinerea*). Overall, the data obtained suggest that CPK32 is a negative regulator in AtPep1-induced immune responses.

Introduction

1.1 The importance of plant immunity

Innate immunity establishes the first line of defense in the host against invading organisms including microbes and predators that can be found in both animals and plants. The innate immunity in plants can contribute to metabolic processes, signaling pathways, interactions of the cells with extracellular environment, molecular recognition, and evolution across biological kingdoms (Jones and Dangl, 2006). The recognition of foreign molecules and anti-microbial defense are to some extent similar between animals and plants (Nürnberger et al., 2004). Like animals, plants are able to recognize foreign molecules derived from microbes, called pathogen-associated molecular patterns (PAMPs). PAMPs are also called elicitors of plant defense that can trigger plant receptor-mediated defense responses against microbes (Nürnberger *et al*., 2004). However, unlike animals, plants are sessile, and lack mobile defender cells and a somatic adaptive immunity (Jones and Dangl, 2006). Thus, plants rely more heavily on innate immunity to defend against pathogens that allows them to grow successfully. The attacking microbes that associate with plant can impair plant growth and reproduction. A detailed understanding and enhancement of plant immune system would be beneficial to agricultural important crops for food, fiber and biofuel production (Huffaker et al., 2006; Jones and Dangl, 2006). In this study, we used *Arabidopsis thaliana* as a model to explore the innate immunity of plants.

1.2 The role of PRRs and Peps in plant defense signaling to coordinate plant immunity

Plants have two steps of the innate immunity: recognition and response. In all plants, many transmembrane pattern-recognition receptors (PRRs) are either receptor kinases (RKs)

or receptor like proteins (RLPs) that have leucine-rich repeats (LRRs) in the extracellular domain and a cytosolic kinase domain (Monaghan et al., 2014). PRRs are essential for plants to detect the presence of the conserved pathogen-associated molecular patterns (PAMPs), which initiates the next step of immune system, defense responses (Ryan et al., 2007). The host PRRs can perceive and bind to these PAMPs, and trigger innate immune responses including an accumulation of antimicrobial proteins and production and recognition of endogenous elicitors, such as *Arabidopsis thaliana* Plant Elicitor Peptide1 (AtPep1). Elicitor peptides can assist in recognition and amplification of immune responses (Huffaker *et al.,* 2006; Ryan *et al.,* 2007; Huffaker et al., 2013). AtPep1 is a 23 amino-acid endogenous peptide that is derived from a 92-amino acid precursor protein AtproPep1(Huffaker *et al.,* 2006). *AtPROPEP1* can be induced by wounding, methyl jasmonate and ethylene (Huffaker and Ryan, 2007). Among the members of Peps family that regulates pathogen resistance responses, AtPep1 was the first discovered. Peps can induce expression of pathogen defense genes and assist in disease resistance when ectopically expressed (Huffaker *et al.,* 2013). AtPep1 can bind to its receptors, PEPR1 and its homolog PEPR2, via the extracellular leucine-rich repeat (LRR) to amplify PAMP-triggered immunity (PTI) (Ryan *et al.*, 2007; Yamaguchi *et al*., 2010; Tang et al., 2015). PEPR1 was first identified on the cell surface of *Arabidopsis* cells using radiolabeled peptide (Yamaguchi *et al.,* 2006). Binding of AtPeps makes PEPR1 or PEPR2 stably associate with the coreceptor, BAK1/SERK3, which is also an LRR receptor-like kinase (Postel *et al.,* 2010; Tang et al., 2015). It was shown that AtPep1 can induce PEPR1LRR-BAK1LRR heterodimerization (Tang *et al.,* 2015). Receptor-like cytoplasmic kinases botrytis-induced kinase 1 (BIK1) also interacts with PEPR1, which it can directly phosphorylated RBOHD to induce ROS production in response to AtPeps (Liu *et*

al., 2013; Kadota *et al.,* 2014). MOB1/CPK28 is also another AtPep/PEPR signaling component that acts as a negative regulator in PTI. CPK28 interacts with and also phosphorylates BIK1. The loss of CPK28 can restore the responsiveness of *bak1/serk3* mutant to PAMPs (Monaghan *et al.,* 2014).

1.3 Phosphoproteomic screen in Arabidopsis identifies proteins that change in phosphorylation state rapidly after Pep treatment

Phosphorylation is an essential post-translational modification of proteins that is responsible for regulating diverse cellular signaling pathways including defense responses. The fact that nearly 4% of the *Arabidopsis* genome encodes serine/threonine protein kinases suggests the importance of phosphorylation as a regulatory mechanism in plants (Ines Lassowskat *et al.*, 2016). Proteogenomics is a method providing orthogonal information and traditional forms of evidence of genome annotation (Walley *et al.,* 2016). This method peptides that are used to refine protein-coding gene models, are identified via tandem mass spectrometry by this method (Walley *et al.,* 2016). Tandem Mass spectrometry with Liquid chromatography (LC-MS/MS) is currently the most suitable technique for analysis of protein phosphorylation in the cell, including identification of phosphoproteins/peptides and determination of the sequence and location of phosphorylation sites (B. A. Garcia *et al.,* 2005; Ines Lassowskat *et al.*, 2016). Since the protein phosphorylation in signaling components is reversible, highly transient, and usually occurs in relatively low level, it is necessary to enrich phosphopeptides before detection via Mass spectrometry (Ines Lassowskat *et al.*, 2016). In this study, phosphoproteomic analysis was done on AtPep1-

treated *Arabidopsis* suspension cells with a treatment time of 10 minutes to identify putative phosphoproteins during early defense response.

1.4 Calcium sensing system and CPK32

One of the candidate phosphopetides identified belongs to the family of calcium-dependent protein kinases. Out of all 34 CPKs, CPK32 was identified to have altered phosphorylation states after AtPep1 treatment. In this study, the role of CPK32 in AtPep1-regulated defense responses was investigated. Calcium ions are ubiquitous second messengers in eukaryotic signal transduction (Schulz *et al.,* 2013). They are one of the most essential ionic species that participate in many biological processes in plants and animals (Gao *et al*., 2014). Many abiotic and biotic stresses and stimuli can trigger the increase in intracellular calcium ion concentration (Schulz *et al.,* 2013). These changes in calcium ion levels will be sensed and translated into intracellular responses through calcium sensor proteins (Gao *et al.*, 2014). Calcium ions have also been shown to be important for the AtPep/PEPR signaling (Qi *et al.,* 2010; Ma *et al*., 2012). Perception of Peps via PEPRs can lead to cytosolic calcium ion elevation, and then CPKs can decode this signal of calcium ion concentration changes in the cytosol to facilitate further immune responses, such as defense gene expression and enhanced resistance to pathogens (Ma et al., 2013). There are two types of calcium sensor proteins. One depends on calcium signals, such as calcineurin B-like/CBL-interacting protein kinases (CBL/CIPKs) and calmodulin proteins (CaMs) (Gao *et al.*, 2014). The other one is sensor protein kinases, such as calcium-dependent protein kinases (CPKs) and calmodulin-dependent protein kinases (CaMKs).

CPKs are proteins that directly bind calcium ions before phosphorylating substrates (Valmonte *et al*., 2014). In plants, CPKs belong to a multigene family, which are primary sensors for detecting the intracellular calcium concentration changes. CPKs translate the changes in calcium concentration into specific phosphorylation events that lead to further downstream signaling pathways (Schulz *et al*., 2013). As shown in Sup. Fig. 1.1, CPKs have a conserved molecular structure, which contains an N-terminal variable domain, a kinase domain with an active site, an auto-inhibitory region, and a calcium-binding domain with four EF-hands (Schulz *et al*., 2013; Day et al., 2002). The *Arabidopsis* genome encodes 34 CPKs. Some of the CPKs have been detected to interact with membrane bound proteins, and most CPKs have a predicted N-myristoylation site involved in membrane targeting (Day et al., 2002). From previous studies, CPK32 is proven to be an essential regulator for plant growth and immune response to abiotic and biotic stress (Zhou *et al*., 2014; Choi *et al*., 2005). Previous studies have identified two phosphorylation sites on CPK32. One is a serine (Ser/S) residue in kinase domain at position 227 (S227), the other one is also a serine residue at position 379 (S379) in the first EF hand following a Threonine residue. Usually, CPKs have a conserved acidic residue, Aspartate (Asp/D), at position 379 (D379) in the first EF hand domain. However, in CPK32 has an S379 residue replacing the conserved acidic D379 residue in the first EF hand. Asp coordinates the calcium ion in the EF hand in most of the CPKs (Sup. Fig. 2.1A and B). The hypothesis is that phosphorylation of this S379 residue represents the switching on of a charge-dependent function in one isoform where the others are constitutively on *(*Nühse *et al., 2004)*.

1.5 *The role of LRR-RLK, SERKS, as co-receptors of PEPRs in plant immune signaling.*

Somatic embryogenesis receptor-like kinases (SERKs) are a leucine rich repeats-receptor like-kinases (LRR-RLKs) sub-family containing five members that play important roles in sensing and translating extracellular signals and initiating cellular responses under various environment challenges (Wu et al., 2015). RLKs have important functions in cell-cell and cell-environment communications (Li, 2010). Similar to RKs, RLKs also have an extracellular domain featuring LRR for ligand-binding, and a cytosolic kinase domain and these domains allow RLKs to perceive the apoplastic signals including phytohormones and small peptides followed by the activation of cytosolic kinase domain, triggering protein phosphorylation cascades as responses (Li *et al.,* 2002; Friedrichsen *et al*., 2000; Wu *et al.,* 2015). SERK1, SERK2, SERK3, and SERK4 are members of SERK sub-family. SERK3/BAK1 is a shared co-receptor of different PRRs including PEPR, EFR, and FLS2 (Yamaguchi and Huffaker, 2011; Postel et al., 2010; Schulze et al., 2010; Heese et al., 2007). The disruption and loss of SERK3 sensitizes and reinforces PEPR signaling at receptor level (Yamada *et al.,* 2015). SERK3 and SERK4 are integral parts of the defense signaling pathways, which incorporate with the LRR-RKs as co-receptor kinases to switch on and off the immune signaling of *Arabidopsis*. SERK4 was identified to have interaction and similar phosphorylation patterns with CPK32. Thus, it is essential to study the function of CPK32 in *Arabidopsis* immunity in relation to SERKs.

Materials and Methods

2.1 Plant materials and growth conditions.

Arabidopsis thaliana Columbia-0 (Col-0) was used as wild-type plants. The *pepr1&2* double mutant (also written as *pepr1/2* in the figures), *cpk32-1* and *cpk32-2* were used as knockout mutants for all bioassays. The *cpk32-1* (SALKseq_139930.2) and *cpk32-2* (SALK_139193) mutant seeds were obtained from *Arabidopsis* Biological Resource Center. The Col-0 and *pepr1&2* double mutant seeds were available in lab. The *pepr1&2* double mutants were first generated in Yamaguchi *et al.* (2010). Seeds sterilization was done in a closed desiccator with chloric gas for 2-4 hours. Chloric gas was made by mixing 50 mL bleach and 1.5 mL concentrated HCl (36.5%-38%) in a beaker placed in then closed desiccator. Seeds were germinated on ½ Murashige and Skoog medium in light controlled growth chamber and transplanted to BM2 soil after 1 week (Growth chamber has 12h light/12 h dark and 22℃).

2.2 Analysis of protein phosphorylation using LC-MS/MS.

Protein phosphorylation data were obtained from UC San Diego Dr. Steve Briggs and Dr. Zhouxin Shen and phsphoproteomic analysis was performed as described in Walley *et al.* (PMC 2016) with modifications. *Arabidopsis* plants were treated with 10 nM AtPep1 and harvested for analysis after 10 minutes. The enriched phosphoproteins were captured using CeO_2 affinity and separated by nano LC using salt gradient on a three-phase capillary column. Analysis of phosphopeptides was made with an LTQ Velos linear ion trap tandem MS in positive ion mode and data-dependent acquisitions. Data were extracted using

Spectrum Mill (Agilent) with peptide abundance and phosphorylation levels quantified by spectral counting.

2.3 Co-expression assays for Mutual Rank

Publicly available RNAseq data was used to probe for strong gene expression correlation. Pairwise measurements of gene co-expression were specified as mutual ranks (MRs; Obayashi and Kinoshita, 2009) (calculated as the geometric mean of the rank of the Pearson's correlation coefficient [PCC] of gene A to gene B and of the PCC rank of gene B to gene A). The MR score for two example genes A and B is given by the formula: $MR_{(AB)} = \sqrt{Rank_{(A\rightarrow B)} \times Rank_{(B\rightarrow A)}}$ where $Rank_{(A\rightarrow B)}$ is the rank of gene B in a PCC-ordered list of gene A against all other genes; similarly, $Rank_{(B\rightarrow A)}$ is the rank of gene A in a PCC-ordered list of gene B against all other genes, with smaller MR scores indicating stronger coexpression between gene pairs (Obayashi and Kinoshita, 2009; Wisecaver *et al.,* 2017).

2.4 Amino acid sequence and Locus number.

The amino acid sequence of CPK32 was obtained from The *Arabidopsis* Information Resources (TAIR). The amino acid sequence alignment of all 34 CPKs was obtained from TAIR Fasta protein sequence.

Atg number

CPK32 (At3g57530)

AtPep1 (At5g64900)

PEPR1 (At1g73080)

PEPR2 (At1g17750)

SERK4 (At2g13790)

SERK3 (At4g33430)

2.5 Arabidopsis Transformation.

Col-0, *pepr1&2, cpk32-1,* and *cpk32-2 Arabidopsis* plants were transformed using the floral dip method with modifications (Clough and Bent, 1998). T1 plants were grown on ½ Murashige and Skoog (MS) agar plates with PPT (10 ng/mL^{-1}). After 2 weeks, resistant plants were transferred to soil.

2.6 Subcellular localization of CPK32.

Transient transformation was done on selected *Nicotiana benthamiana* leaves with agrobacterium using syringe infiltration. Agrobacterium was transformed with an AtCPK32-YFP plant expression vector and p19 silencing inhibitor vector. The infiltrated leaves were visualized under microscope for YFP expression after 2-5 days.

2.7 Yeast-2-hybrid transformation and cloning.

The coding region of the kinase domains of SEKR4 and PEPR1 and whole CPK32 was PCR-amplified using specific primers (Primers are listed in Table 1). The amplified fragments were cloned into the pENTR D-TOPO vector and later transferred by recombination to the destination vectors pAS and pACT. The proteins were fused to both GAL4 DNA binding domain (DBD) and GAL4 activation domain (AD) in the vectors pAS and pACT, respectively. The desired pairs of the pAS and pACT vectors were co-transformed into yeast strain AH109 using the lithium acetate/single-stranded carrier

DNA/PEG (LiAc/SSDNA/PEG) method, as described by Gietz and Woods (2006). Transformed yeast cells were selected on a synthetic complete medium lacking leucine, tryptophan, histidine and tryptophan for 3 to 4 days at 28 °C.

2.8 Peptide elicitor treatment

The stock of AtPep1 is 1 mM and it was diluted with miliQ water to 1 μM for each treatment. Stock of AtPep1 is available in the lab. Treatments were performed as described in Huffaker *et al.*, 2013 with modifications. Modifications are described in each assay.

2.9 Root Growth Inhibition and Seedling Growth Inhibition measurement.

1μM of AtPep 1 was added into ½ Murashige and Skoog medium. For root growth inhibition assay, sterile seeds were added in two lines using sterile toothpicks in each square petri dish plate (~15-18 seeds per line per genotype). Each plate was taped and seeds were stratified at 4°C for 3 days and moved to growth chamber for germination. After 10 days, pictures of the plates were taken and root length was measured using Image J. For seedling growth inhibition assay, sterile seeds were spread evenly onto ½ MS medium plate and stratified seeds at 4°C for 3 days and moved to growth chamber for germination. Seedlings were transferred into liquid ½ MS medium with 1μM of AtPep 1 after 3 days of germination. After 7-9 days, the fresh weight of each plant was measured.

2.10 Luminol-based ROS Detection and Measurement.

The assay was performed as described in Smith and Heese (2014) with modifications. Plants used for this assay were about 3-week-old. Two leaf disks were added to each well of

a 96 well plate with each well containing 150 µL of ddH_2O, 24 hours prior to conducting a ROS assay. For total six plants, one leaf per plant and two leaf disks per leaf were pooled. Two leaf disks were randomly selected from different plant and placed into one well. (Incubated the plate) The plate was incubated at room temperature (22°C) in constant light, with the adaxial side of the disks facing upwards reduces the wounding response. Water was removed from each well prior to treatment. 100 µL of elicitor or control solution were added into each well using a multichannel pipette. Reaction mixture contained 20 µg/mL HRP, 34 µg/mL Luminol (prepared freshly in 200 mM of KOH), and 1 µM AtPep1 or equal volume of water for control solution. The plate was placed without delay into a BioTek Synergy H1 microplate reader (La Jolla, California, USA) to measure AtPep1-induced ROS production between 0 and 40 minutes.

2.11 MAPK Activation assay

Two-week-old seedlings were treated with 1 µM of AtPep1 and then harvested in liquid nitrogen after 0, 2, 5, 10, 15, and 30 minutes. Proteins were extracted with lacus buffer (50 mM Tris–HCl pH 7.5, 10 mM $MgCl_2$, 15 mM EGTA, 100 mM NaCl, 1 mM sodium fluoride, 1 mM sodium molybdate, 0.5 mM activated Na_3VO_4, 30 mM beta-glycero-phosphate, 0.1% TritonX 100). The homogenized protein samples were centrifuged at 21000 rcf for 20 min at 4°C. 5x SDS loading buffer was added into each supernatant sample and subjected to immunoblot analysis.

2.12 Western-Blot Analysis.

Extracted protein samples with 1x SDS loading buffer were loaded on 10% SDS-PAGE gel. Two sets of two layers of Whatman paper and one layer of nitrocellulose membrane were used for blotting the protein with semi-dry transfer buffer. Protein was blocked for MAPK activation detection with 5% BSA. Wash the protein with 1x TBS-T after primary antibody and secondary antibody incubation and then with 1x TBS after secondary antibody. Primary antibody for MAPK activation detection was Anti-MPK 1:3,000 in 5% BSA p44/42 MAPK (Erk1/2) Antibody #9102, for YFP detection was anti-YFP 1:4,000 in 0.1% non-fat milk. Secondary antibody for both MAPK activation detection and YFP detection was Anti-rabbit HRP 1:5,000 in 0.1% non-fat milk. The protein was incubated with each antibody solution for one hour at room temperature or overnight at 4°C. Antibodies were purchased from Cell Signaling Technology Company or Thermo Fisher. Bio-Rad precision plus protein™ dual xtra standards was used as protein ladder. Gel image of immunoblots was taken with Bio-Rad Molecular Imager Chemioc™ XRS+ imaging system. Ponceau-S stain was used for loading control to detect RuBisCo (~52kDa). RubisCo is an enzyme in chloroplast that involves in photosynthesis.

2.13 Isolation of RNA and expression analysis by RT-qPCR.

Two-week-old seedlings were treated with 1 µM of AtPep1 or water as control and then harvested in liquid nitrogen after 18 hours. Total 4 samples per genotype per time point and 8 seedlings per sample were used. Total RNA of each sample was isolated from the plant samples using Trizol reagent (Trisure, by Bioline) following Chromczynski and Sacchi (1987) protocol. For each isolated RNA sample, 20 µL RNA was purified using DNase I, RNase free (Invitrogen EN0521 by Thermo Fisher Scienctific). RNA integrity was checked

on freshly prepared agarose gel after purification and DNase digestion. For each sample, 2 μg of purified RNA was reverse-transcribed using the M-MLV reverse transcriptase kit following the manufacturer's instructions (Invitrogen). Quantitative PCR was performed with Bio-Rad CFX96 real-time PCR detection system (Bio-Rad). The expression levels of genes of interest were normalized to those of a reference gene, Actin2 (At3g18780). *PDF1.2* gene was used as defense marker for AtPep1 dependent induction. Representative results of three or more independent experiments with at least three biological replicate each are shown. The trial with 18-hour samples has only been done for once for a different time-point than 24-hour.

2.14 Pseudomonas syringae infection assay.

The assay was performed as described by Katagiri *et al.* (2002) with modifications. Bacteria are streaked out from a -80°C glycerol stock onto a plate of low salt Luria Bertani (LB) medium (pH=7.0) with 50 μg/mL Rifampicin (1×Rif) and 25 μg/mL Cycloheximide (1×CHX). The bacteria were grown in dark at 28°C for 2 day and then transferred to a 20 mL liquid low salt LB medium with 1× Rif and grown with shaking at 28°C for 12 hours. The overnight culture reached mid to late log phase growth ($0.6<OD_{600}<1.0$). The bacteria from half of the culture were harvested by centrifugation of 2500 rcf for 10 minutes at room temperature. The bacteria pellet was resuspended with10 mM $MgCl_2$. Then the resuspension of bacterial cells was diluted to a lower level of inoculum for syringe infiltration (OD_{600}=0.0002 of *Pst* DC3000 is 1×10^5 cfu/mL). Total six plants per genotype, three leaves per plant and one leaf per time-point (0, 2, 5 days after infection) were pooled. Selected leaves were marked and fully infiltrated with 1-mL needleless syringe containing the diluted

bacterial suspension on the abaxial side. After the infiltrated leaves were dry, leaf disks from 0 days after infection (dai) were harvested and the plants were covered with a plastic dome to maintain humidity. Two leaf disks were cut from one leaf with a size 2 cork borer (~6.35mm in diameter), total 12 leaf disks per genotype per time-point. Randomly selected 2 leaf disks into one biological replicate sample to make total six biological replicates per genotype per time-point. The tissue samples were ground with plastic beads in 1 mL 96-deep-well plate with 300 µL of 10 mM $MgCl_2$. A 30 µL of sample is removed and diluted in 270 µl of $MgCl_2$. A serial of seven 1:10 dilution series were made for each sample by repeating this process (Dilution factors: 10^0, 10^{-1}, 10^{-2}, 10^{-3}, 10^{-4}, 10^{-5}, 10^{-6},10^{-7}). An aliquot of 10 µL of the 1:10 dilutions were spotted on low salt LB medium with Rif and CHX. The plates were placed in the dark at 28°C for 2 days and then the colony forming units for each dilution of each sample were counted.

2.15 Botrytis cinerea infection assay.

This assay was performed as described by Berr *et al*. (2010) with modifications. The *Botrytis cinerea* was grown on V8 juice agar (200mL: 72 mL V8 juice, 0.4g $CaCO_3$, 4g bacterial agar) plate for a week at 25 °C. Spores were harvested using a sterile Q-tip and resuspended in BD Difco Potato Dextrose broth (Becton, Dickinson and Company, 0.96g PDB in 40 mL sterile miliQ water) containing 0.1% Tween 20 at a density of 1 to 5×10^5 spores/mL, and incubated for 2 hours at 25 °C - 28 °C before inoculation. Then, 5 µL spore suspensions were dropped on the adaxial surface of rosette leaves, where the leaves were previously wounded with a needle. About 3-4 leaves per plant were inoculated with the

fungus, and 16 plants per genotype were used. The lesions were visible 2 days after infection, and measured 3 days after infection using Image J.

2.16 Statistical Analyses.

Each experiment was done at least 3 independent times with similar results. Graphs are used from the most representative trial. One portion of data had statistical significances based on unpaired two sample student's *t*-test were determined with Graph Pad QuickCalcs. Another portion of data had statistical significance based on one-way ANOVA with Tukey HSD multiple comparison.

Results

3.1.1 CPK32-YFP was Transiently Expressed in N. benthamiana.

AtCPK32-YFP fusion was transiently expressed in transgenic *N. benthamiana* plants under control of 35S promoter. The YFP was fused to the C-terminal end of the CPKs to avoid disrupting a putative N-terminal acylation signal. From the transient expression in *N. benthamiana* leaves, the C-terminal YFP fusion protein (CPK32-YFP) presented at the periphery of the cells, as revealed by confocal microscopy (Fig. 1.1 A). The result suggests that CPK32 has a similar localization with PEPRs at the plasma membrane. This expression was observed in multiple independent transgenic lines (data not shown). The presence of CPK32-YFP was confirmed in Western blot protein detection with antibody, anti-YFP 1:4,000 (Fig. 1.1 B).

3.1.2 CPK32 had Highly Similar Phosphorylation Pattern with SERK4 and interacted with PEPR co-receptor, SERK4.

From the result of transient expression of CPK32-YFP in N. *benthamiana* plants, CPK32 is suspected to be in close proximity to PEPR1 within the cell. To further explore the relation between CPK32 and other components of the PEPR signaling, a gene co-expression assay for mutual rank and protein-protein interaction detections were done. The co-expression network was constructed from a publicly available RNAseq data. The mutual ranks of the gene expression correlation showed that at least seven genes had the similar gene expression patterns with CPK32 (Fig. 1.2 A). Among the seven genes, only *SERK4* was observed to be differentially phosphorylated after AtPep1 treatment and involved in plant defense immunity. Thus, *SERK4* was suspected to relate to CPK32 in Peps-induced immunity. The protein-

protein interaction assay was done using CPK32, and the cytosolic kinase domain of SERK4, SERK3 and PEPR1 using yeast-two-hybrid (Y2H) system (Fig. 1.2B). Although CPK32 was indicated to have similar localization with PEPRs, the yeast-two-hybrid protein-protein interaction detection showed that CPK32 did not interact with PEPR1. From previous literatures, BAK1/SERK3 was indicated as a shared co-receptor for many different PRRs including PEPRs in plants (Yamada et al., 2015; Yamaguchi and Huffaker., 2011). Both SERK3 and SERK4 were determined to genetically cooperate to achieve full signaling capability in response to AtPep1 (Roux et al., 2011). SERK4, as a co-receptor of PEPRs, has highly similar gene expression patterns with CPK32 (Fig. 1.2A). Thus, the interactions between CPK32 and SERK4, and CPK32 and SERK3 were checked with yeast-two-hybrid in *vivo*. The yeast-two-hybrid protein-protein interaction assay showed that CPK32 interacted with SERK4, but not SERK3 (Fig. 1.2 B). The interactions between SERK4 and PEPR1, SERK3 and PEPR1 were also confirmed (Fig1.2 B). The empty vectors were used as negative controls. Although CPK32 did not show interaction with PEPR1 nor SERK3, it showed interaction with one of the PEPR1 co-receptors, SERK4. Thus, CPK32 may indirectly interact with PEPR1 via SERK4.

3.2 CPK32 did not affect Seedling and Root growth of Arabidopsis thaliana in Response to AtPep1.

In previous study, CPK32 was demonstrated as a regulator of ABA signaling pathways, which were responsive for vegetative growth of plants (Choi et al., 2005). Thus, CPK32 may participate in seedling growth and root growth (Fig. 1.2). From the phosphoproteomic analysis data, CPK32 was differentially phosphorylated after AtPep1 treatment, which

implies that CPK32 is a part of the AtPep1-induced signaling. We hypothesized that if CPK32 is involved in growth and development of plants, the growth responses to AtPep1 might be altered in *cpk32* mutants. In this case, the *cpk32* mutant lines may have a different sensitivity to AtPep1 comparing to Col-0 *Arabidopsis*. To test this hypothesis, a root growth inhibition analysis was carried out. Roots from Col-0 plants were sensitive to AtPep1 and their growth was inhibited at low μM level of AtPep1. The negative control *pepr1&2* was insensitive to AtPep1 (Fig. 2.1A and B). However, the *cpk32* mutants did not significantly change the sensitivity to AtPep1 compared to Col-0. Col-0 and *cpk32* mutants had similar root growth (lower than 20%) when comparing the root length after AtPep1 treatment versus water (mock) treatment (Fig. 2.1A and B). To further confirm this result, seedling growth inhibition analysis was performed (Fig. 2.1C). Similar to the results of root growth inhibition analysis, the negative control *pepr1&2* was insensitive to 1 μM AtPep1, but the Col-0 and *cpk32* mutants had similar seedling growth around 20% when comparing the root length after AtPep1 treatment versus water (mock) treatment (Fig. 2.1C). The *cpk32* mutants had similar level of sensitivity to Col-0 in response to 1 μM AtPep1 in root growth and seedling growth assays.

3.3.1 The Absence of CPK32 Affected AtPep1-Induced Rapid ROS production.

Although CPK32 had no direct effect on AtPep1-inhibited plant growth, CPK32 is still suspected to participate in some other AtPep1-induced defense responses. To test whether CPK32 has a direct role in AtPep1 signaling, AtPep1/PEPRs- mediated early responses were examined in *cpk32* mutants. The rapid and transient accumulation of apoplastic reactive oxygen species is one of the best characterized and robust early AtPep1-induced signaling

events (Smith and Heese, 2014). Col-0 plants responded rapidly to 1 μM AtPep1 with induction of an oxidative burst (Fig. 3.1A). The negative control *pepr1&2* double mutant has no response to AtPep1 with no significant induction of oxidative burst. This ROS response was clearly increased in *cpk32* mutants with much higher ROS burst peaks at about 7-minute (420-second) time-point relative to Col-0 plants (Fig. 3.1A). The maximum ROS production at 420-second (7-min) timepoint indicates that *cpk32* mutants had significantly higher ($p<0.01$) ROS peaks relative to maximum ROS released by Col-0 plants (Fig. 3.1 B). These results indicate that *cpk32* mutants are hypersensitive to peptide in the ROS signaling.

3.3.2 The Absence of CPK32 Affected AtPep1-Induced Rapid MAPK activities.

Similar to rapid ROS production, the activation of mitogen-activated protein kinase (MAPK) cascades is also an important mechanism of plant early immune response to elicitors (Lee et al., 2004). AtPep1 can stimulate the rapid activation of at least 2 MAPKs referred to as AtMPK3 and AtMAPK6. To further explore the effect of CPK32 on AtPep1-induced early immune responses, Col-0, *pepr1&2*, and *cpk32* mutants were treated by AtPep1 and the MAPK activity in each genotype was analyzed by Western Blot. Anti-p44/42 MAPK (Erk1/2) was used as antibody to detect activated MAPKs. The negative control *pepr1&2* had no MAPK activity at any time-point in response to 1 μM AtPep1 (Fig. 3.2). Col-0 and *cpk32* mutants started to have MAPK activity 5 minutes after 1 μM AtPep1 treatment and MAPK activity decreased after 15 minutes of treatment. The *cpk32* mutants had higher activation of MAPK at 5- and 15-minute time-points comparing to that of Col-0 (Fig. 3.2). This result showed that rapid signals of MAPK activation in response to AtPep1

was increased in the absence of CPK32. Thus, CPK32 may negatively affect AtPep1-induced activation of MAPK cascade.

3.3.3 CPK32 Controls AtPep1-Induced Defense Related Gene Expression.

To elucidate the effects of CPK32 on AtPep1/PEPR-regulated pathways, qRT-PCR analysis was done on Col-0, *pepr1&2*, and *cpk32* mutant seedlings that were exposed to 1 μM AtPep1 for two different time-points, 18-hour with 0-hour as a no-treatment control. The AtPep1-induced defense related gene chosen for this assay was *PDF1.2*. The *PDF1.2* gene in *Arabidopsis* encodes a plant defensin, and it is usually used to characterize jasmonate/ethylene-dependent responses (Brown et al., 2003). From previous studies of AtPep1-induced defense responses, *PDF1.2* expression was strongly induced by AtPep1 in Col-0 plants (Huffaker and Ryan, 2007). Thus, we are interested in how absence of CPK32 affects the relative expression of *PDF1.2* in *Arabidopsis* upon AtPep1 treatment. Both of the *cpk32* mutants appeared to have significantly higher *PDF1.2* relative expressions than that of Col-0 plants at 18-hour (Fig3.3). The *pepr1&2* was a negative control that has extremely low *PDF1.2* relative expressions in response to AtPep1 (Fig. 3.3). This result shows that AtPep1-induced *PDF1.2* relative expressions was increased in the absence of CPK32. Therefore, CPK32 may negatively affect the AtPep1-induced *PDF1.2* relative expressions in *Arabidopsis.*

3.4 CPK32 Affects Disease Phenotypes and Basal Resistance to Bacterial Pathogens in Arabidopsis.

After characterizing CPK32 in AtPep1-induced early and rapid immune responses in *Arabidopsis*, the role of CPK32 in pathogen resistance was assessed. Two different pathogens were used to infect the plant samples. *Pseudomonas syringae* pv. *tomato* DC3000 (*Pst* DC3000) is a hemibiotrophic bacterial pathogen and *Botrytis cinerea* is a necrotrophic fungal pathogen (Zhang et al., 2015). *P. syringae* can infect wide variety of plants, so they are known for diverse and host-specific interactions with plants (Hirano and Upper, 2000). The effect of CPK32 in immunity against *Pst* DC3000 was examined by comparing the bacterial growth in infected leaves of Col-0 and *cpk32* mutants with 1 μM of AtPep1 pretreatment and *pepr1&2* as a negative control. Pretreatment with peptide was shown to induce protective defense responses that limit *Pst* DC3000 proliferation (Zipfel et al., 2004; Yamaguchi et al., 2010). Thus, AtPep1 pretreatment enhanced the differences in resistance to *Pst* C3000 among different genotypes that have different resistance to *Pst* DC3000. The *cpk32* mutants had clearly less colonies grown on low salt LB medium within the same dilutions (Fig. 4.1A). The bacterial growth rates in infected leaves of Col-0 and *cpk32-1* were Log_{10}(7.4408) CFU/cm^2 and Log_{10}(6.5327) CFU/cm^2 at 5 dai, respectively, resulting in ~55 folds of decrease in bacterial growth in the *cpk32* mutants relative to the Col-0 plants (Fig. 4.1B). The *cpk32* mutants had significantly lower bacterial growth relative to Col-0 plants in proliferation of *Pst* DC3000 with a p-value smaller than 0.01 (Fig. 4.1B).

Botrytis cinerea is a very destructive plant pathogen that attacks wide range of crops worldwide. Due to its necrotrophic lifestyle, *B. cinerea* causes serious losses to numerous crop species. Thus, it is a key model for studying plant immunity against necrotrophic fungi (Williamson et al., 2007). The effect of CPK32 in immunity against *B. cinerea* was examined by comparing the disease phenotype (leaf lesion) in infected leaves of Col-0 and *cpk32*

mutants. Lesions caused by *B. cinerea* infection were clearly visible on all infected spots after 3 days of infection. The lesion developed most extremely in *pepr1&2* mutant plants and least extreme in *cpk32* mutant plants (Fig. 4.1C and D). The *cpk32* mutants had significant smaller lesion area relative to Col-0 plants with a p-value smaller than 0.01 (Fig. 4.1D). The absence of CPK32 decreased the susceptibility and increased the resistance of the plants against both bacterial and fungal pathogens in *Arabidopsis*. Thus, CPK32 is suggested to negatively affect the plants resistance to plant pathogens. The results are consistent to the effect of CPK32 on AtPep1-induced early immune responses.

Discussion

To further study Pep-induced signaling pathways in plants immunity, we want to explore novel components in Pep-regulated immune signaling. The preliminary data of phosphoproteomic analysis showed that CPK32 was differently phosphorylated after AtPep1 treatment, which led us to characterize CPK32 in AtPep1-induced immunity. Calcium ions are ubiquitous second messengers in cytoplasmic region of eukaryotic cells and they have important role in translating extracellular signals into various signaling pathways (Schulz et al., 2013). Calcium dependent protein kinase (CPK) is one of the calcium sensors that have essential roles in regulation of plant growth and development and as well as responses to biotic and abiotic stresses (Zou et al., 2010). *Arabidopsis* encodes 34 CPKs, and some of them were shown to have function in immune signaling responses (Schulz et al., 2013; Zou et al., 2010). Previously, CPK32 was identified as a component of the abscisic acid (ABA) signaling that regulated stress-responsive gene expression during vegetative growth. CPK32 could auto- and trans-phosphorylate other substrates to induce defense responses in *Arabidopsis* (Choi et al., 2005). In this study, CPK32 was characterized and identified as an important regulatory component in response to AtPep1. The results presented demonstrate that CPK32 negatively regulates PEPRs signaling pathways probably via co- receptor, SERK4, in *Arabidopsis.*

CPK32 is a plasma membrane protein that participates in PEPRs regulated pathways via co-receptor, SERK4.

The transient expression of YFP tagged CPK32 in *N. benthamiana* leaves was visualized and captured under microscope. CPK32-YFP was found at the periphery of the cells, which

suggested that CPK32 has the same localization to the membrane bound PRRs, PEPR1 and PEPR2 (Fig. 1.2 A). The presence of CPK32-YFP was also confirmed using Western blot protein detection (Fig 1.1 B). Previous studies also indicate that CPK32 has subcellular targeting signals at membrane and in the nucleus (Choi et al., 2005*)*. In the near future, a co-localization of CPK32-YFP and PEPR1-mCherry should be done to see if they are in close proximity to each other via SERK4. To further explore the relationship of CPK32 with other components in PEPR signaling, co-expression analysis was constructed from a global RNAseq dataset to identify genes that have highly correlated expression pattern as *CPK32*. *SERK4* was one of the genes that have similar expression pattern with CPK32 (Fig. 1.2 A). SERK4 was the only one that participates in immune signaling and shows an altered phosphorylation state after AtPep1 treatment. Thus, the interaction between CPK32 and SERK4 was checked using yeast-two-hybrid assay. The yeast-two-hybrid result indicated that CPK32 interact with SERK4, but neither with PEPR1 nor SERK3. PEPR1 showed interaction with both SERK4 and SERK3 (Fig. 1.2 B). The interactions between CPK32 and SERK4 suggested that CPK32 is suspected to participate in PEPRs signaling via co-receptor, SERK4. Since the yeast-two-hybrid protein interaction assay was done using the entire coding region of CPK32, it will be also important to check if the kinase domain and the first EF-hand of CPK32 that have S227 and S379 phosphorylation sites respectively interact with SERK4 individually. S227 and S379 were shown to be phosphorylated after peptide treatment in our phosphoproteomic data. Thus, further protein-protein detection with CPK32 variants of phosphomimetic (S227D, S379D) and phosphoabolishing lines (S227A and S379A) should be used to reveal if CPK32 interacted with SERK4 through active kinase domain and/or first EF-hand. A Yeast-three hybrid assay could also be done on CPK32,

SERK4 and PEPR1 together to confirm if CPK32 interact with PEPR1 via SERK4. CPK32 may also interact with PEPR1 *in planta*, so biomolecular fluorescence complementation (BiFC) analysis or co-immunoprecipitation (Co-IP) assays in *planta* should also be done to check if CPK32 and the CPK32 phosphovariants interacts with PEPR1, SERK3, and SERK4.

CPK32 has redundant function in AtPep1 inhibited root growth and seedling growth.

In previous studies, CPK32 was identified as a regulator of ABA signaling, which is responsible for vegetative growth of plants (Choi et al., 2005). Thus, we were interested in the effect of CPK32 on the inhibition of plant growth and development by AtPep1. In this study, the results show that *cpk32* mutants displayed no obvious difference from Col-0 on AtPep1 generated inhibition of root growth and seedling growth (Fig. 2.1). The previous studies of CPKs demonstrate that the close homology in CPK subfamilies might cause functional redundancy in some signaling pathways (Schulz et al., 2013; Mori et al., 2006). However, CPK32 belongs to *Arabidopsis* CPK subgroup II and is only closely related to CPK14 (Day *et al.,* 2002). CPK14 has not been identified for any function in previous studies of CPK, so it is not clear if there are other CPKs having functional redundancy with CPK32. Thus, one hypothesis is that CPK32 does not regulate defense limited growth. The second hypothesis is that there may be other proteins that substitute CPK32 in *cpk32* mutants in AtPep1-induced root growth inhibition and seedling growth inhibition. Another hypothesis is that CPK32 may regulate root and seedling growth inhibition in different PRRs-mediated pathways other than PEPRs.

*CPK32 acts as a negative regulator in AtPep1-induced early defense signaling***.**

The recognition and perception of PAMPs and DAMPs can lead to various downstream signaling events in *Arabidopsis.* The early immune responses are activation of downstream defense responses. These early defense reactions include the rapid generation of ROS, rapid MAPK activity and altered defense-related gene expression. These rapid biochemical reactions were induced by AtPep1 usually occur within several minutes to a few hours after treatment with AtPep1. The rapid production of ROS burst by RBOHD oxidase is a conserved signal response in plant immunity (Kadota et al., 2014). In this study, the rapid AtPep1-induced ROS production bursts were significantly higher in the absence of CPK32 (Fig. 3.1 A). The total ROS accumulation throughout 40-minute period was also significantly higher in *cpk32* mutants compared to Col-0. Thus, CPK32 is suspected to function as a negative regulator in AtPep1-induced rapid ROS production. BIK1, as a direct substrate of PEPR1, can directly phosphorylates NADPH oxidase RBOHD to mediate ROS production upon perception of AtPep1. BIK1-mediated RBOHD phosphorylation is calcium independent, but PAMP-induced RBOHD is globally dependent on calcium signaling, the calcium-regulated activation of RBOHD may be subsequent of that of BIK1 (Kadota *et al.,* 2014). Since CPK32 interact with PEPRs- SERK4 complex via SERK4, CPK32 might directly or indirectly attenuate the activation of RBOHD downstream of BIK1 phosphorylation of RBOHD. However, in order to further endorse this claim, the interaction and phosphorylation between CPK32 and RBOHD, and CPK32 and BIK1 still need to be checked using Y2H, CoIP and/or LC-MS/MS. Second, CPK23 was suspected to have a negative effect on AtPep1-induced rapid MAPK activity. The perception and recognition of diverse foreign molecules by PRRs lead to pattern-triggered immunity (PTI) to defend plants from pathogens. The activation of MAPK is an important mechanism for plants to establish

disease resistance to pathogens (Bi et al., 2018; Lee et al., 2004). Previous studies of PRRs and MAPK cascades indicate that all PRRs activate two MAPK cascades, the one that is composed of two MKKs, MKK4 and MKK5, and two MAPKs, MPK3 and MPK6, is more essential to regulate plant immunity (Asai et al., 2002; Gao et al., 2008; Bi *et al*., 2018). In this study, AtPep1-triggered MAPK activity is stronger in the absence of CPK32. Thus, CPK32 is suspected to negatively regulate the MAPK cascades in PEPR signaling. One hypothesis is that the presence of CPK32 might trigger the activation of a phosphatase of the MAPK signaling cascades. The phosphatase can lead to partial loss of the MAPK activities. Third, one of the major roles of AtPep1 is to amplify PAMP signals through inducing defense-related genes in *Arabidopsis* (Huffaker and Ryan, 2007). Previous studies of CPKs indicate that CPKs can decode the intracellular calcium ion changes into defense gene expression changes (Ma et al., 2013). To examine the effect of CPK32 on defense response gene expression in PEPR signaling, *PDF1.2* was chosen as the target defense-related gene and Actin2 was chosen as a reference gene. AtPep1 can activate the transcription of *PDF1.2* gene encoding a plant defensin through jasmonate/ethylene signaling pathways (Huffaker and Ryan, 2007). In this study, the qRT-PCR results demonstrate that *cpk32* mutants have significantly higher relative expression of *PDF1.*2 at both 18-hour post AtPep1 induction comparing to Col-0 plants (Fig. 3.3). The results suggest that the presence of CPK32 may suppress or decrease the transcription of *PDF1.2* in response to AtPep1. Together the evidence suggests that CPK32 is a negative regulator of AtPep1.

CPK32 acts as a negative regulator in Arabidopsis resistance to plant pathogens.

To study if CPK32 has any biological relevance, the effect of CPK32 in plant resistance to bacterial pathogens was examined using *Pst* DC3000 and *B. cinerea*. The PEPR signaling shares some of the same signaling pathways as PAMPs leading to basal resistance. Pretreatment of AtPep1 also enhances resistance to fungal and bacterial pathogens (Huffaker et al., 2006, Huffaker and Ryan, 2007). Since we were characterizing CPK32 in AtPep/PEPR signaling, it is necessary to study the effect of CPK32 on AtPep1 enhanced plant resistance to pathogens. Moreover, *Pst* DC3000 is modulated via the salicylic acid (SA)-mediated signaling, and *B. cinerea* is modulated via JA/ET-mediated signaling, and AtPep1 is an amplifier of both signaling pathways (Zhang et al., 2015; Huffaker and Ryan, 2007). In this study, the results of *Pst* DC3000 infection assay with 1 μM AtPep1 pretreatment show that there was a significant reduction of bacterial growth in *cpk32* mutants relative to wild-type Col-0 (Fig. 4.1A and B). Thus, CPK32 may act as a negative regulator in AtPep1 enhanced resistance to *P. syringae* in *Arabidopsis*. The similar results were found on *B. cinerea* infection assay without AtPep1 pretreatment. The *cpk32* mutants displayed much smaller lesion size relative to wild-type Col-0 plants (Fig. 4.1C and D). The data showing the lesion area of 12 individual plants per line suggested that *cpk32* mutants are significantly more resistant to *B. cinerea* than wild-type Col-0 plants (Fig. 4.1D). The presence of CPK32 may impair PTI signaling. Therefore, CPK32 is suspected to negatively regulate the *Arabidopsis* resistance to bacterial and fungal pathogens.

Together with all the characterization of *cpk32* mutants in this study, which exhibit enhanced DAMP- and PAMP-triggered immune responses, it can be concluded that CPK32 is a regulator of DAMP- and PAMP-triggered immunity. The mechanism of how CPK32

regulate these immune signaling pathways is still unclear. In this regard, it is essential to study the effect of phosphorylation of CPK32 on early immune signaling and resistance to plant pathogens. Transgenic lines with phosphomimetic and phosphoabolishing mutations at the sites observed to change in phosphorylation post-AtPep1 treatment have been generated and homozygous mutants are currently being selected. Two phosphorylation sites, S227 and S379, in the kinase domain and first EF-hand respectively were replaced by Alanine (Ala/A) and Asp. The double knockout mutants of *cpk32-1* with *serk4*, *serk3 and pepr1&2* are also on selection. The next step is to apply these transgenic lines and double knockout mutant lines to these bioassays to further elucidate the function of CPK32 in AtPep1-induced immunity.

Figures

A.

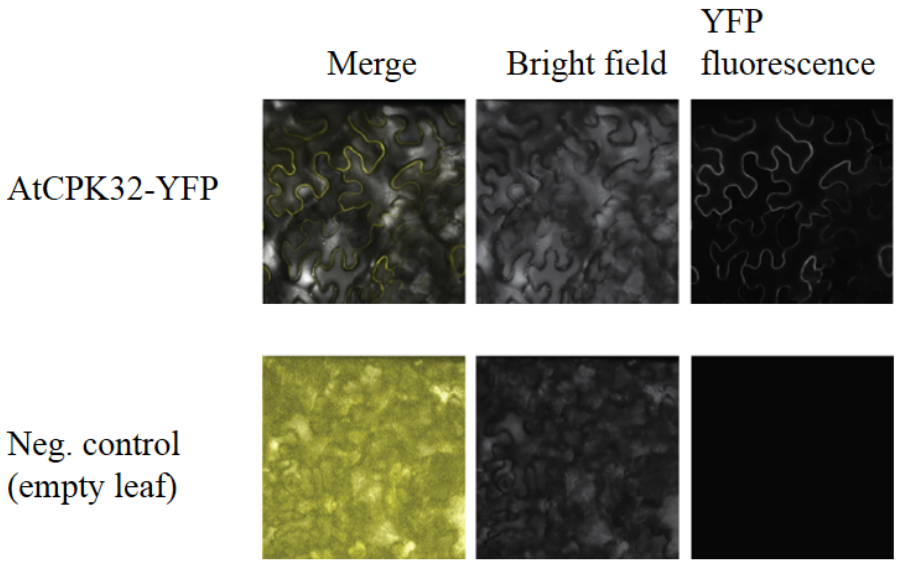

B.

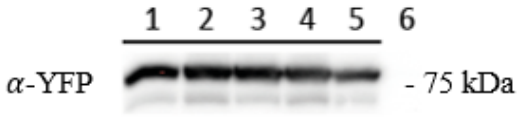

1-CPK32
2-CPK32 kinase dead
3-CPK32(S227A)
4-CPK32(S227D)
5-CPK32(S379A)
6-Empty *N. benthamiana* leaf

Fig. 1.1 Subcellular distribution of C-terminal 35S::YFP fusion CPK32 in the leaf of *N. benthamiana.* The C-terminal 35S::YFP fusion CPK32 was transiently expressed in *N. benthamiana* leaves by agro-infiltration. Leaf sections were inspected by confocal microscopy 3 d after infiltration. (A) CPK32-YFP was transiently expressed in the leaf of *N. benthamiana* at plasma membrane of the cell. An empty leaf of *N. benthamiana* was also presented as a negative control with no YFP expression. (B) The presence of CPK32-YFP in the leaf of *N. benthamiana* was confirmed using Western blotting protein detection.

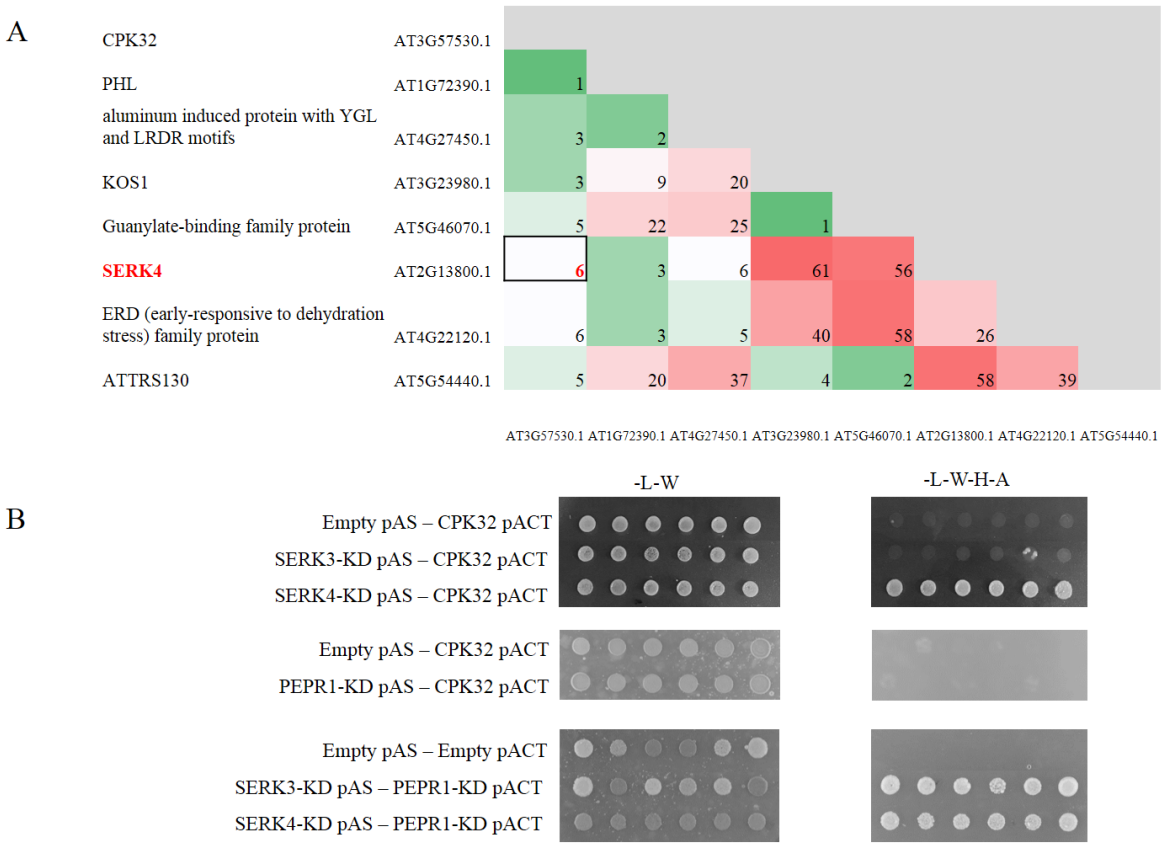

Fig. 1.2 The correlation and interaction between CPK32 and SERK4 were shown in co-expression assay and yeast-two-hybrid assay. (A) The co-expression results were analyzed using RNAseq Pearson's correlation and presented in mutual ranks. (B) The entire coding region of CPK32 and the coding region of kinase domain of PEPR1, SERK3 and SERK4 was fused to both GAL4 DNA-binding domain and GAL4 activation domain in the vectors DBD (pAS) and AD (pACT), respectively. The transformed yeast cells were selected on a synthetic complete medium lacking leucine, tryptophan, histidine and adenine to test interactions. Empty pAS vector was used as a negative control and vectors combination of SERK3-KD pAS_PEPR1-KD pACT was used as a positive control. This assay was performed three times with similar results.

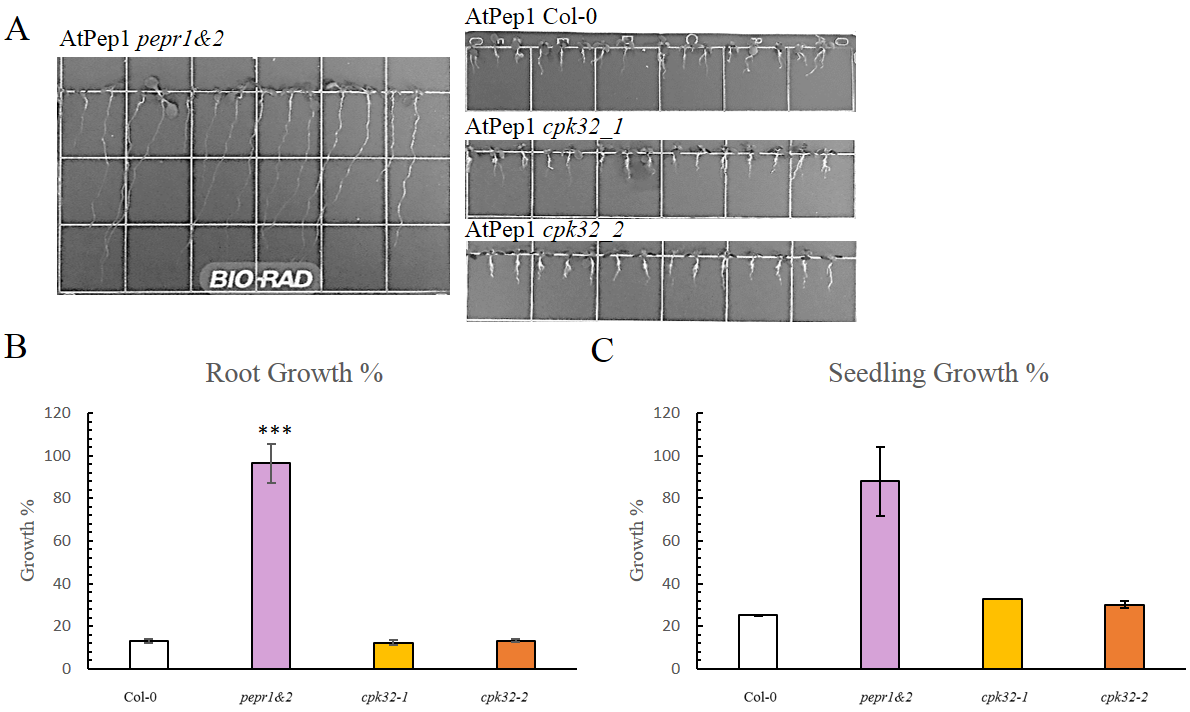

Fig. 2.1 AtPep1 inhibition of primary root growth and seedling growth in Col-0, *cpk32-1, cpk32-2*, and *pepr1&2* mutant seedlings. (A) Roots of one-week-old Col-0, *cpk32-1, cpk32-2*, and *pepr1&2* mutant seedlings on ½ MS agar plate containing 1 µM AtPep1. The width of the square grind line is 1.3cm/200 pixels used as scale bar. Representative seedlings are shown for 1 µM AtPep1 treatment. (B) Root growth percentage of one-week-old Col-0, *cpk32-1, cpk32-2*, and *pepr1&2* mutant seedlings. Root growth percentage was calculated as (the length of root in 1 µM AtPep1)/ (the length of root in water treatment) *100. The error bars represent SEM, and the asterisks indicate a statistical difference between Col-0 and mutants (*** $P < 0.001$ by Student's T-test). (C)Seedling growth percentage of two-week-old Col-0, *cpk32-1, cpk32-2*, and *pepr1&2* mutant seedlings. Seedlings were weighed and the weight of each seedling were recorded in mg as each data point. Seedling growth percentage was calculated as (the weight of seedling in 1 µM AtPep1)/ (the weight of seedling in water treatment) ×100. The error bars represent SEM. Although the growth % of the mutants were not significantly different from that of Col-0 by using student's T-test (2 tailed p-Value=0.0593), from the dataset, *pepr1&2* has 2 fold more of growth % than Col-0 and *cpk32* mutants, which indicates *pepr1&2* is a valid negative control in this data.

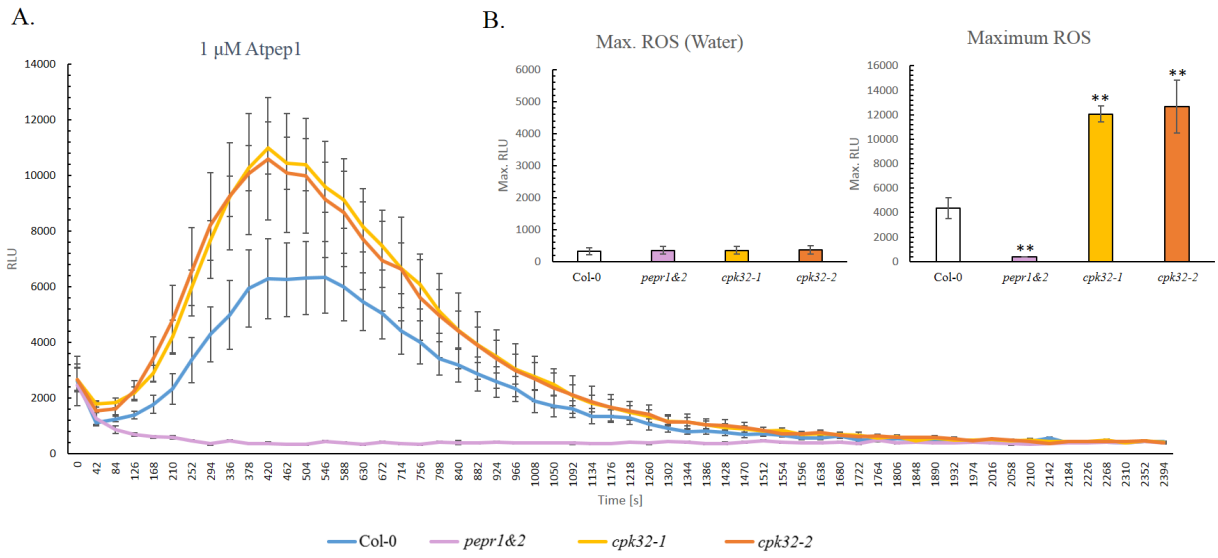

Fig. 3.1 AtPep1-Induced Early Immune Response, Rapid ROS Production by RBOHD, in Col-0, *pepr1&2, cpk32-1,* and *cpk32-2* mutants. ROS production was measured continuously with cut and pre-incubated leaf disks using luminol bioassay. (A) The ROS production of 3-Week-Old Col-0, *cpk32-1, cpk32-2*, and *pepr1&2* mutants was monitored during a 40-min measurement after addition of 1 µM AtPep1. (B) The maximum ROS emission in relative light units was calculated from ROS emission at 420s of each genotype (Two-way ANOVA, **=p<0.01)

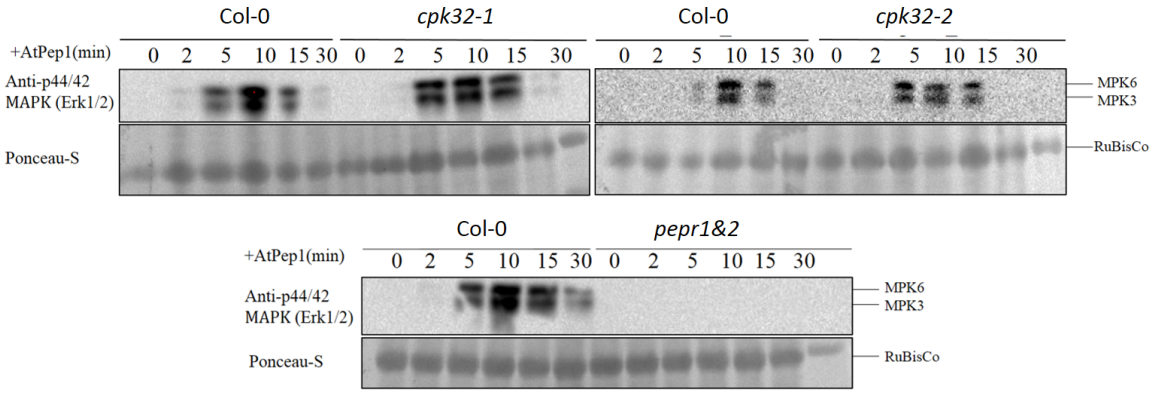

Fig. 3.2 AtPep1-Induced Early Immune Response, rapid MAPK activation, in Col-0, *pepr1&2, cpk32-1,* and *cpk32-2* mutant seedlings. Seedlings of Col-0, *pepr1&2, cpk32-1* and *cpk32-2* mutants were growing in 1/2 MS liquid medium for 2 weeks and treated with 1 μM AtPep1 for indicated time periods. Proteins were detected by Western blotting using the indicated antibodies. Ponceau S-stained is shown as a loading control.

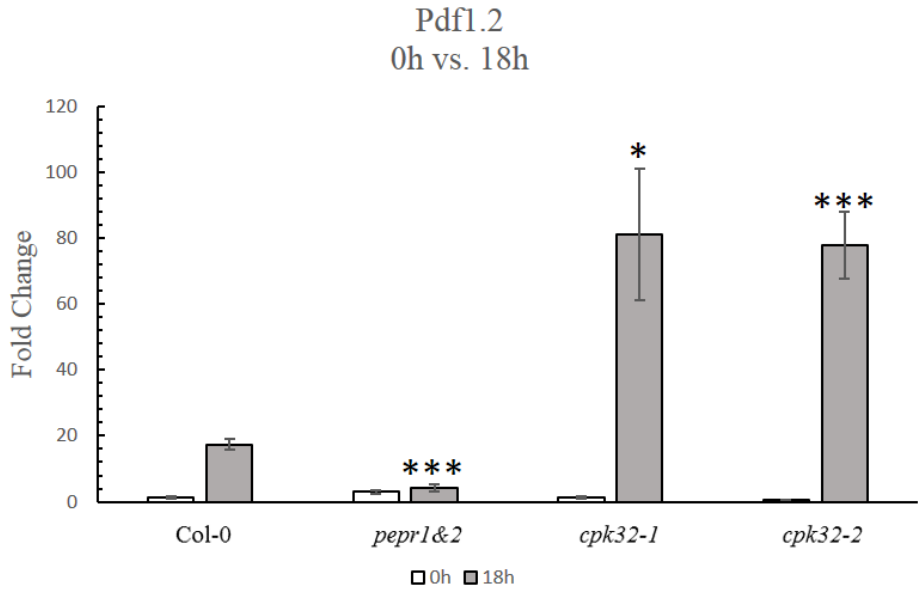

Fig. 3.3 Expression analysis of AtPep1-inducible defense related gene, *PDF1.2*, in 2-week-old Col-0, *cpk32-1, cpk32-2*, and *pepr1&2* mutant seedlings. Plants were germinated in ½ MS agar medium for 7 days and then transferred into liquid ½ MS medium for another 7 days. Plants were treated with AtPep1 (1 µM) for 18 hours (grey bars). Untreated plants are indicated as 0 hours as controls. *ACTIN2* expression was used as a reference gene for internal control. Error bars represent standard errors between 4 individual biological replicates. Asterisks indicate statistical differences between treated mutants and treated Col-0 (Student's T-test, *=p<0.05, **=p<0.01, ***=p<0.001)

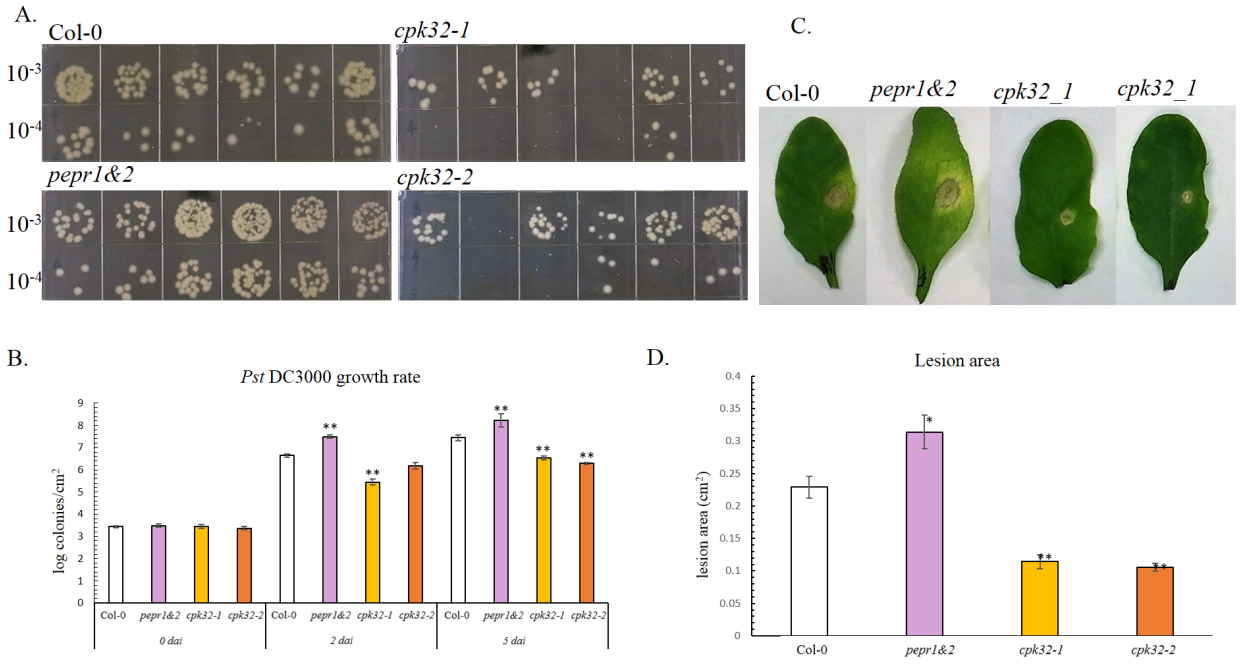

Fig. 4.1 Plant pathogen infection assays: the phenotypes of plant pathogen infected Col-0 and *cpk32* mutants. *Pst* DC3000 infection assay of Col-0, *cpk32-1, cpk32-2, and pepr1/pepr2* mutants pretreated with 1 µM AtPep1 24 hours before inoculation and inoculated with low level of *Pst* DC3000 (OD600=0.0002 of *Pst* DC3000 is 1 x 10^5 cfu/mL). (A) *Pst* DC3000 colonies of diluted leaf samples in 10 nM of $MgCl_2$ that are collected 2 days post infection with dilution factors of 10^3 and 10^4. (B) *Pst* DC3000 proliferation in Col-0, *cpk32-1, cpk32-2, pepr1&2* with 1 µM AtPep1 0, 2, and 5 days post infection. Values presented are the average ± SE from 6 individuals bio-replicates (ANOVA, **=p<0.01). (C) and (D) *B. cinerea* infection assay. The disease lesion 3 days after infection is shown by representative leaves. The lesion diameter was measured using ImageJ. Values presented are the average ± SE from 4 individuals bio-replicates and each bio-replicate contains 3 lesion disks from 3 individual plants (Two-way ANOVA, **=p<0.01, *p<0.05).

Tables

Table 1.1 Primer List.

Gene name	Sequence	Primer name and useage	Length (bp)	TA	Amplicon (bp)	Gene ID
AtCPK32	ACGCATCTTGCATCAGTTTG	SALKseq_139930.2-LP Genotyping T-DNA insertion	20	49 °C	1061	At3g57530
AtCPK32	GCTTGATCCTGACCAAAAGC	SALKseq_139930.2-RP Genotyping T-DNA insertion	20	51 °C		
AtCPK32	TTGCATCCCTTTGATTCAATC	SALK_139193-LP Genotyping T-DNA insertion	21	48 °C	1156	At3g57530
AtCPK32	TCAGGAAAATGCTTGATCCTG	SALK_139193-RP Genotyping T-DNA insertion	21	50 °C		
SERK4	TGGCTCAGAAGAAAACCACAG	SALK_057955.48.75-LP Genotyping T-DNA insertion	21	52 °C	1152	At2g13790
SERK4	TGGCTCAGAAGAAAACCACAG	SALK_057955.48.75-RR Genotyping T-DNA insertion	21	52 °C		
AtActin2	TCCCTCAGCACATTCCAGCAGAT	Actin2-q-F qPCR	23	56 °C		At3g18780
AtActin2	AACGATTCCTGGACCTGCCTCATC	Actin2-q-R	24	58 °C		
AtPDF1.2	CTTATCTTCGCTGCTCTTGT	PDF1.2-qRT-PCR-Fw_2 qPCR	20	49 °C	205	At5g44420
AtPDF1.2	CGTAACAGATACACTTGTGTGC	PDF1.2-qRT-PCR-Rv_2 qPCR	22	52 °C		
AtCPK32	TGGACACAAGCCAAAGAGGG	AtCPK32-q-F3 qPCR	20	53 °C		At3g57530
AtCPK32	CGATGTCTCCAGCATCCATCA	AtCPK32-q-R3 qPCR	21	53 °C		

Table 1.1 Primer List (continued).

Cutinase	GATGTGACGGTCATCTTTGCCC	Bc-Cut-A (Z69264) F qPCR	22	56 °C		
Cutinase	AGATTTGAGAGCGGCGAGG	Bc-Cut-A (Z69264) R qPCR	19	52 °C		
PEPR1	CACCATGCTAAATGAAAAGTACACC	AtPEPR1-KD-Y2H-F Yeast-two-hybrid cloning	25	54 °C		At1g73080
PEPR2	TTACCGAACTGAATCAGAGGAG	AtPEPR1-KD-Y2H-R Yeast-two-hybrid cloning	22	52 °C		
CPK32	CACCATGGGTAATTGTTGCGGAACA	AtCPK32 F1 Yeast-two-hybrid cloning and YFP fusion	25	57 °C	1617	At2g57530
CPK32	TCATCTTGTATCACCATTGAC	AtCPK32 R1 Yeast-two-hybrid cloning	21	48 °C		
CPK32	TCTTGTATCACCATTGACCTG	AtCPK32 R2 YFP fusion	21	50 °C	1614	
BAK1 (SERK3)	CACCATGCGAAGGAAAAAGCCGCAG	BAK1-KD-Y2H-F Yeast-two-hybrid cloning	25	60 °C		At4g33430
BAK1 (SERK3)	TTATCTTGGACCCGAGGGG	AK1-KD-Y2H-R Yeast-two-hybrid cloning	19	52 °C		
BAK7(SERK4)	CACCATGCTCAGAAGAAAACCACAGGACC	BAK7-KD-Y2H-F Yeast-two-hybrid cloning	29	52 °C		At2g13790
BAK7(SERK4	TTATCTTGGACCCGAGGG	BAK7-KD-Y2H-R Yeast-two-hybrid cloning	18	62 °C		

Supplemental Figures

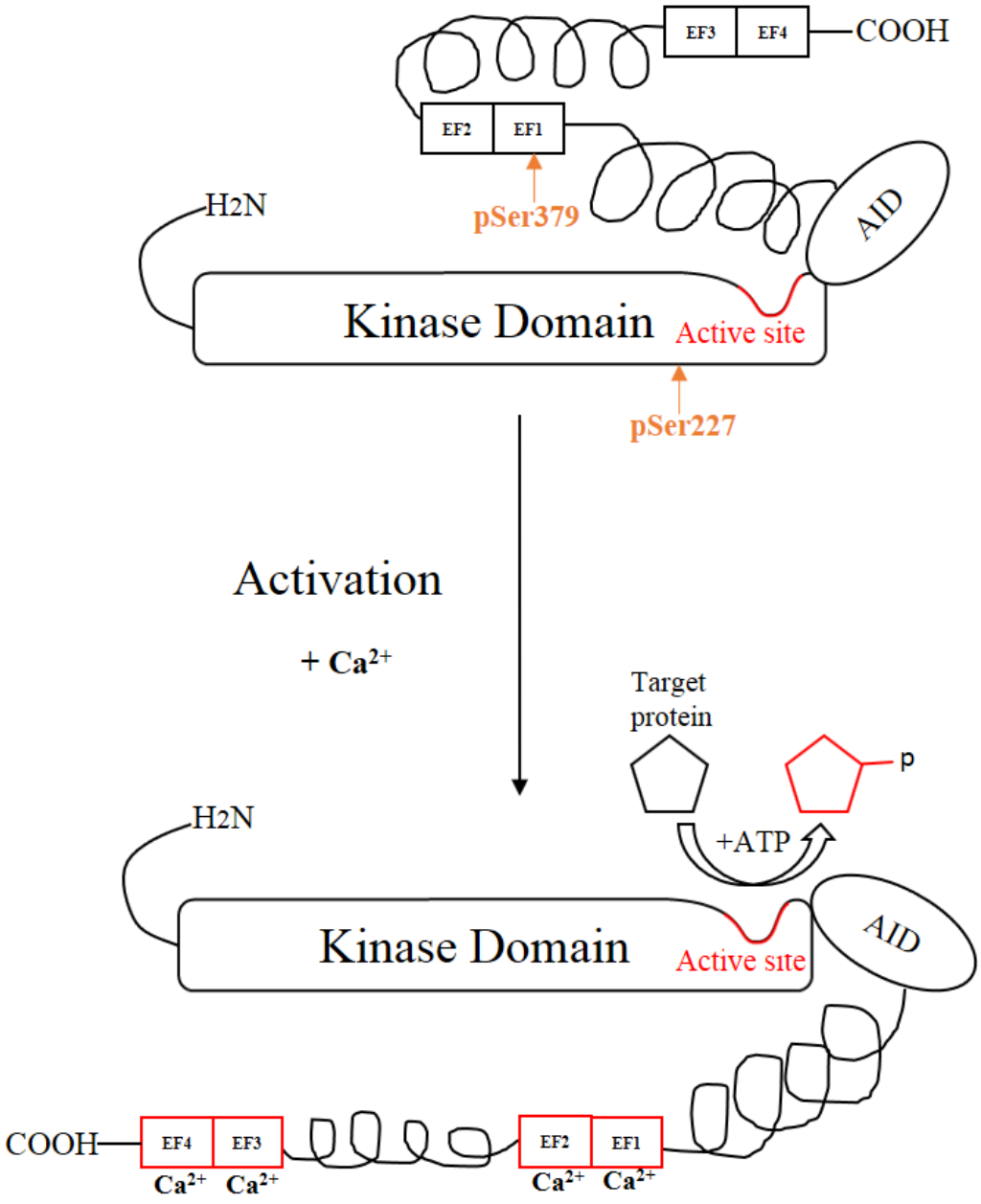

Sup. Fig. 1.1 Scheme of CPK32 Modular structure and activation. CPK32 modular structure contains an N-terminal domain, a kinase domain with an active site, a calcium binding domain with 2 alpha-helices and 4-EF hands, and an auto-inhibitory domain between the kinase domain and calcium binding domain. CPK activation occurs when Ca^{2+} bind to 4-EF hands, which induces conformational changes leading to the exposure of the active site. The exposure of active site allows CPK to autophosphorylate and phosphorylate other target substrates.

A

```
  1 MGNCCGTAGS LAQNDNKPKK GRKKQNPFSI DYGLHHGGGD GGGRPLKLIV
 51 LNDPTGREIE SKYTLGRELG RGEFGVTYLC TDKETDDVFA CKSILKKKLR
101 TAVDIEDVRR EVEIMRHMPE HPNVVTLKET YEDEHAVHLV MELCEGGELF
151 DRIVARGHYT ERAAAAVTKT IMEVVQVCHK HGVMHRDLKP ENFLFGNKKE
201 TAPLKAIDFG LSVFFKPGER FNEIVGSPYY MAPEVLKRNY GPEVDIWSAG
251 VILYILLCGV PPFWAETEQG VAQAIIRSVL DFRRDPWPKV SENAKDLIRK
301 MLDPDQKRRL TAQQVLDHPW LQNAKTAPNV SLGETVRARL KQFTVMNKLK
351 KRALRVIAEH LSDEEASGIR EGFQIMDTSQ RGKINIDELK IGLQKLGHAI
401 PQDDLQILMD AGDIDRDGYL DCDEFIAISV HLRKMGNDEH LKKAFAFFDQ
451 NNNGYIEIEE LREALSDELG TSEEVVDAII RDVDTDKDGR ISYEEFVTMM
501 KTGTDWRKAS RQYSRERFNS ISLKLMQDAS LQVNGDTR
```

Sup. Fig. 2.1 Amino acid sequence of all 34 CPKs with position 379 and amino acid sequence of CPK32. (A) The amino acid sequence of CPK32. The kinase domain and first EF-hand domain are underlined respectively. The active site in the kinase domain is highlighted in grey. The 2 phosphorylation-sites S227 and S379 are in red. (B) CPK32 has a phosphoserine replacing the conserved Aspartate at position 379 is in red and highlighted in grey.

Sup. Fig. 2.1 Amino acid sequence of all 34 CPKs with position 379 and amino acid sequence of CPK32 (continued).

B

```
CPK18 RALAKTINEDELDDLRDQFDAIDIDKNGSISLEEMRQALAKDVPWKLKDARVAEI
CPK16 RALATTLDEEELADLRDQFDAIDVDKNGVISLEEMRQALAKDHPWKLKDARVAEI
CPK28 RALASTLDEAEISDLRDQFDAIDVDKNGVISLEEMRQALAKDLPWKLKDSRVAEI
CPK24 RIVADNLPNEEIAAIVQMFQTMDTDKNGHLTFEELRDGLKKIGQ-VVPDGDVKML
CPK7  RVIAEHLSVEEAAGIKEAFEMMDVNKRGKINLEELKYGLQKAGQ-QIADTDLQIL
CPK8  RVIAEHLSVEEVAGIKEAFEMMDSKKTGKINLEELKFGLHKLGQQQIPDTDLQIL
CPK14 RVIAEHLSVEETSCIKERFQVMDTSNRGKITITELGIGLQKLGI-VVPQDDIQIL
CPK32 RVIAEHLSDEEASGIREGFQIMDTSQRGKINIDELKIGLQKLGH-AIPQDDLQIL
CPK15 LEHPWIRGGEAPDKPIDSAVLSRMKQFRAMNKLKKLALKVIAES-LSEEEIKGLK
CPK13 RVIAEFLSTEEVEDIKVMFNKMDTDNDGIVSIEELKAGLRDFST-QLAESEVQML
CPK10 RVIAEHLSIQEVEVIKNMFSLMDDDKDGKITYPELKAGLQKVGS-QLGEPEIKML
CPK30 RVIAEHLSIQEVEVIRNMFTLMDDDNDGKISYLELRAGLRKVGS-QLGEPEIKLL
CPK25 RVIAERLSEEEIHELRETFKTIDSGKSGRVTYKELKNGLERFNT-NLDNSDINSL
CPK20 KVIAESLSEEEIAGLKEMFKMIDTDNSGHITLEELKKGLDRVGA-DLKDSEILGL
CPK2  RVIAESLSEEEIAGLKQMFKMIDADNSGQITFEELKAGLKRVGA-NLKESEILDL
CPK1  RVIAESLSEEEIAGLKEMFNMIDADKSGQITFEELKAGLKRVGA-NLKESEILDL
CPK26 RVIAESLSEEEIAGLKEMFKAMDTDNSGAITFDELKAGLRRYGS-TLKDTEIRDL
CPK6  KVIAESLSEEEIAGLRAMFEAMDTDNSGAITFDELKAGLRRYGS-TLKDTEIRDL
CPK5  KVIAESLSEEEIAGLREMFQAMDTDNSGAITFDELKAGLRKYGS-TLKDTEIHDL
CPK12 RVIAERLSEEEIGGLKELFKMIDTDKSGTITFEELKDSMRRVGS-ELMESEIQEL
CPK11 RVIAERLSEEEIGGLKELFKMIDTDNSGTITFEELKAGLKRVGS-ELMESEIKSL
CPK4  RVIAERLSEEEIGGLKELFKMIDTDNSGTITFEELKAGLKRVGS-ELMESEIKSL
CPK3  KVIAENLSEEEIIGLKEMFKSLDTDNNGIVTLEELRTGLPKLGS-KISEAEIRQL
CPK17 RVIAGCLSEEEIMGLKEMFKGMDTDSSGTITLEELRQGLAKQGT-RLSEYEVQQL
CPK34 RVIAGCLSEEEIMGLKEMFKGMDTDNSGTITLEELRQGLAKQGT-RLSEYEVQQL
CPK29 KVIAENLSEEEIKGLKQTFKNMDTDESGTITFDELRNGLHRLGS-KLTESEIKQL
CPK31 KVIAANLSEEEIKGLKTLFTNIDTDKSGTITLEELKTGLTRLGS-NLSKTEVEQL
CPK27 KFIAANLSEEEIKGLKTLFTNIDTDKSGNITLEELKTGLTRLGS-NLSKTEVEQL
CPK22 KVIAEGLSEEEIKGLKTMFENMDMDKSGSITYEELKMGLNRHGS-KLSETEVKQL
CPK19 KFIAQNLKEEELKGLKTMFANMDTDKSGTITYDELKSGLEKLGS-RLTETEVKQL
CPK33 KVIAENIDTEEIQGLKAMFANIDTDNSGTITYEELKEGLAKLGS-RLTEAEVKQL
CPK9  KVIAENIDTEEIQGLKAMFANIDTDNSGTITYEELKEGLAKLGS-KLTEAEVKQL
CPK23 KVSAVSLSEEEIKGLKTLFANMDTNRSGTITYEQLQTGLSRLRS-RLSETEVQQL
CPK21 KVIAESLSEEEIKGLKTMFANIDTDKSGTITYEELKTGLTRLGS-RLSETEVKQL
```

References

Asai, T., Tena, G., Plotnikova, J., Willmann, M. R., Chiu, W-L., Gomez-Gomez, L., Boller, T., Ausubel, F. M. AND Sheen, J. 2002. MAP kinase signalling cascade in *Arabidopsis* innate immunity. *Nature* volume415, pages977–983

Berr A, McCallum EJ, Alioua A, Heintz D, Heitz T, Shen WH. 2010. Arabidopsis histone methyltransferase SET DOMAIN GROUP8 mediates induction of the jasmonate/ethylene pathway genes in plant defense response to necrotrophic fungi. *Plant Physiology* 154, 1403–1414.

Brown, R. L., Kazan, K., McGrath, K. C., Maclean, D. J. and Manners, J. M. 2003. A Role for the GCC-Box in Jasmonate-Mediated Activation of the *PDF1.2* Gene of *Arabidopsis*. *Plant Physiology* Vol. 132, Issue 2. DOI: https://doi.org/10.1104/pp.102.017814

Choi, H., Park, H-J., Park, J. H., Kim, S., Im, M-Y., Seo, H-H., Kim, Y-W., Hwang, I. and Kim, S. Y. 2005. *Arabidopsis* Calcium-Dependent Protein Kinase AtCPK32 Interacts with ABF4, a Transcriptional Regulator of Abscisic Acid-Responsive Gene Expression, and Modulates Its Activity. *Plant Physiology* 139: 1750–1761. DOI: https://doi.org/10.1104/pp.105.069757
Chromczynski, P. and Sacchi N. 1987. Single-step method of RNA isolation by acid guanidinium thiocyanate-phenol-chloroform extraction. *Anal Biochem* 162(1):156-9. DOI: 10.1006/abio.1987.9999

Clough, S. J. and Bent, A. F. 1998. Floral dip: a simplified method for Agrobacterium-mediated transformation of *Arabidopsis thaliana*. The Plant Journal (1998) 16(6), 735–743
Dangl, J. L. and Jones, J. D. G. 2006. The plant immune system. *Nature* 444, 323–329

Day, I. S., Reddy, V. S., Ali, G. S. and Reddy, A. 2002. Analysis of EF-hand-containing proteins in *Arabidopsis*. *Genome Biology* 3: research 0056.1. Available at: https://doi.org/10.1186/gb-2002-3-10-research0056

Friedrichsen, D. M., Joazeiro, C. A., Li, J ., Hunter, T. and Chory, J. 2000. Brassinosteroid-insensitive-1 is a ubiquitously expressed leucine-rich repeat receptor serine/threonine kinase.
Gao, M., Liu, J., Bi, D., Zhang, Z., Cheng, F., Chen, S. and Zhang, Y. 2008.MEKK1, MKK1/MKK2 and MPK4 function together in a mitogen-activated protein kinase cascade to regulate innate immunity in plants. *Nature News*. Available at: https://www.nature.com/articles/cr2008300.

Gao, X., Jr., K. C. and He, P. 2014. Functions of Calcium-Dependent Protein Kinases in Plant Innate Immunity. *Plants* 3, 160–176. doi:10.3390/plants3010160

Garcia, B. A., Shabanowitz, J. and Hunt, D. F. 2005. Analysis of protein phosphorylation by mass spectrometry. *Methods* 35, 256–264. doi:10.1016/j.ymeth.2004.08.017

Gietz, R.D., and Woods, R. A. 2006. Transformation of yeast by the liac/ss carrier DNA/PEG method. *Methods Mol Biol.* 313: 107–120. pmid:16118429

Heese, A., Hann, D. R., Gimenez-Ibanez, S., Jones, A. M., He, K., Li, J., Schroeder, J. I., Peck, S. C. and Rathjen, J.P. 2007. The receptor-like kinase SERK3/BAK1 is a central regulator of innate immunity in plants. *Proc Natl Acad Sci* USA, 104, pp. 12217-12222

Hirano, S. S. and Upper, C. D. 2000. Bacteria in the Leaf Ecosystem with Emphasis on *Pseudomonas syringae*—a Pathogen, Ice Nucleus, and Epiphyte. *Microbiol Mol Biol Rev.* 64(3): 624–653. PMCID: PMC99007

Huffaker, A. Pearce, G., Veyrat, N., Erb, M., Turlings, Ted C. J., Sartor, R., Shen, Z., Briggs, S. P., Vaughan, M. M., Alborn, H. T., Teal, Peter E. A., and Schmelz, E. A. 2013. Plant elicitor peptides are conserved signals regulating direct and indirect antiherbivore defense. *PNAS.* doi/10.1073/pnas.1214668110.

Huffaker, A., Gregory, P., and Ryan, C. A. 2006. An Endogenous Peptide Signal in *Arabidopsis* Activates Components of the Innate Immune Response. *PLOS Biology*, Public Library of Science, doi.org/10.1073/pnas.0603727103.

Huffaker, A.; Ryan, C. A. 2007. Endogenous peptide defense signals in *Arabidopsis* differentially amplify signaling for the innate immune response. *Proceedings of the National Academy of Sciences*. 104 (25) 10732-10736. https://doi.org/10.1073/pnas.0703343104

Kadota, Y., Sklenar, J., Derbyshire,P., Stransfeld, L., Asai, S., Ntoukakis, V., Jones, J. DG., Shirasu, K., Menke, F., Jones, A. and Zipfel, C. 2014. Direct Regulation of the NADPH Oxidase RBOHD by the PRR-Associated Kinase BIK1 during Plant Immunity. *Molecular Cell* 54, 43–55. http://dx.doi.org/10.1016/j.molcel.2014.02.021

Katagiri, F., Thilmony, R. and He, S.Y. 2002 The *Arabidopsis thaliana*-pseudomonas syringae interaction. *Arabidopsis Book* 1:e0039. doi: 10.1199/tab.0039.

Lassowskat, I., Hoehenwarter, W., Lee, J. & Scheel, D. 2016. Phosphoprotein Enrichment Combined with Phosphopeptide Enrichment to Identify Putative Phosphoproteins During Defense Response in *Arabidopsis thaliana*. *Methods in Molecular Biology Environmental Responses in Plants* 373–383. doi:10.1007/978-1-4939-3356-3_30

Lee, J., Rudd, J. J., Macioszek, V. K. and Scheel, D. 2004. Dynamic Changes in the Localization of MAPK Cascade Components Controlling Pathogenesis-related (*PR*) Gene Expression during Innate Immunity in Parsley. *The Journal of Biological Chemistry* 279, 22440-22448. doi: 10.1074/jbc.M401099200

Li, J. 2010. Multi-tasking of somatic embryogenesis receptor-like protein kinases. *Curr.Opin.PlantBiol.* Vol. 13. Issue 5. p.509-541. https://doi.org/10.1016/j.pbi.2010.09.004

Li, J., Wen, J., Lease, K. A., Doke, J. T., Tax, F. E. and Walker, J. C. 2002. BAK1, an *Arabidopsis* LRR Receptor-like Protein Kinase, Interacts with BRI1 and Modulates Brassinosteroid Signaling. Cell Press, Volume 110, Issue 2, Pages 213-222. https://doi.org/10.1016/S0092-8674(02)00812-7

Liu, Z., Wu, Y., Yang, F., Zhang, Y., Chen, S., Xie, Q., Tian, X. and Zhou, J-M. 2013. BIK1 interacts with PEPRs to mediate ethylene-induced immunity. *PNAS.* 110 (15) 6205-6210; https://doi.org/10.1073/pnas.1215543110

Ma, Y., Walker, R. K., Zhao, Y., Berkowitz, G. A. 2012. *Linking ligand perception by PEPR pattern recognition receptors to cytosolic Ca2+ elevation and downstream immune signaling in plants*. *Proc Natl Acad Sci USA*; **109**:19852–19857.

Ma, Y., Zhao, Y., Walker, R. K. and Berkowitz, G. R. 2013. Molecular Steps in the Immune Signaling Pathway Evoked by Plant Elicitor Peptides: Ca^{2+}-Dependent Protein Kinases, Nitric Oxide, and Reactive Oxygen Species Are Downstream from the Early Ca^{2+} Signal. *Plant Physiology* 163(3): 1459–1471. doi: 10.1104/pp.113.226068

Monaghan, J., Matschi, S., Shorinola, O., Rovenich, H., Matei, A., Segonzac, C., Malinovsky, F. G., Rathjen, J. P., MacLean, D., Romeis, T., Zipfel, C. 2014. The Calcium-Dependent Protein Kinase CPK28 Buffers Plant Immunity and Regulates BIK1 Turnover. *PLOS Biology*, Public Library of Science, doi.org/10.1016/j.chom.2014.10.007.

Mori, I. C., Murata, Y., Yang, Y., Munemasa, S., Wang, Y. F., Andreoli, S., Tiriac, H., Alonso, J. M., Harper, J. F., Ecker, J. R., et al. (2006) CDPKs CPK6 and CPK3 function in ABA regulation of guard cell S-type anion- and Ca2+-permeable channels and stomatal closure. *PLoS Biol* 4: e327

Nühse, T. S., Stensballe, A., Jensen O. N. and Peck, S. C. 2004. Phosphoproteomics of the *Arabidopsis* Plasma Membrane and a New Phosphorylation Site Database. *The Plant Cell* Vol. 16, No. 9 pp. 2394-2405. Available at: https://www.jstor.org/stable/3872380. Access provided by University of California San Diego.

Nürnberger, T., Brunner, F., Kemmerling, B., Piater, L. 2004. Innate Immunity in Plants and Animals: Striking Similarities and Obvious Differences. *Freshwater Biology*, Wiley/Blackwell (10.1111), onlinelibrary.wiley.com/doi/pdf/10.1111/j.0105-2896.2004.0119.x.

Obayashi, T., Kinoshita, K. 2009. Rank of correlation coefficient as a comparable measure for biological significance of gene coexpression. *DNA Res*. 16: 249–260.
Plant Physiol., 123, pp. 1247-1256

Postel, S., Küfner, I., Beuter, C., Mazzotta, S., Schwedt, A., Borlotti, A., Halter, T., Kemmerling, B. and Nürnberger, T. 2010. The multifunctional leucine-rich repeat receptor kinase BAK1 is implicated in *Arabidopsis* development and immunity. European Journal of Cell Biology. Volume 89, Issues 2–3, Pages 169-174. https://doi.org/10.1016/j.ejcb.2009.11.001

Qi, Z., Verma, R., Gehring, C., Yamaguchi. Y., Zhao, Y., Ryan, C. A. and Berkowitz, G. A. 2010. *Ca2+ signaling by plant Arabidopsis thaliana Pep peptides depends on AtPepR1, a receptor with guanylyl cyclase activity, and cGMP-activated Ca2+ channels*. *Proc Natl Acad Sci USA*; **107**:21193–21198.

Ross, A., Yamada, K., Hiruma, K., Yamashita-Yamada, M., Lu, X., Takano, Y., Tsuda, K., Saijo, Y. 2014. The *Arabidopsis* PEPR Pathway Couples Local and Systemic Plant Immunity. *The EMBO Journal*, EMBO Press, emboj.embopress.org/content/33/1/62.

Roux, M., Schwessinger, B., Albrecht, C., Chinchilla, D., Jones, A., Holton, N., Malinovsky, F. G., Tör, M., Vries, S. de, Zipfel, C., 2011. The *Arabidopsis* Leucine-Rich Repeat Receptor–Like Kinases BAK1/SERK3 and BKK1/SERK4 Are Required for Innate Immunity to Hemibiotrophic and Biotrophic Pathogens. *The Plant Cell*, Vol. 23: 2440–2455. DOI: https://doi.org/10.1105/tpc.111.084301

Ryan, C. A., Huffaker, A., Yamaguchi, Y. 2007. New insights into innate immunity in *Arabidopsis*. *Cellular Microbiology* 9(8), 1902–1908, doi:10.1111/j.1462-5822.2007.00991.x

Schulz, P., Herde, M. and Romeis, T. 2013. Calcium-Dependent Protein Kinases: Hubs in Plant Stress Signaling and Development. *Plant Physiology* 163: 523–530. DOI: https://doi.org/10.1104/pp.113.222539

Schulze, B., Mentzel, T., Jehle, A.K., Mueller, K., Beeler, T., Boller, S., Felix, G. and Chinchilla, D. 2010. Rapid heteromerization and phosphorylation of ligand-activated plant transmembrane receptors and their associated kinase BAK1. J Biol Chem, 285. pp. 9444-9451

Smith, J. M. and Heese, A. 2014. Rapid bioassay to measure early reactive oxygen species production in *Arabidopsis* leave tissue in response to living *Pseudomonas syringae*. *Plant Methods* 10:6. https://doi.org/10.1186/1746-4811-10-6

Tang, J., Han, Z., Sun, Y., Zhang, H., Gong X. and Chai, J. 2015. Structural basis for recognition of an endogenous peptide by the plant receptor kinase PEPR1. *Cell Research* 25:110–120. doi: 10.1038/cr.2014.161

Valmont. G. R., Arthur. K., Higgins. C. M. and MacDiarmid R. M. 2014. Calcium-dependent protein kinases in plants: evolution, expression and function. *Plant Cell Physio l*55(3):551-69. doi: 10.1093/pcp/pct200.

Walley, J. W. and Briggs, S. P. 2016. Dual use of peptide mass spectra: Protein atlas and genome annotation. *Current Plant Biology* 2:21-24. https://doi.org/10.1016/j.cpb.2015.02.001

Williamson, B., Tudzynski, B., Tudzynski, P. and Kan, J. A. L. V. 2007. *Botrytis cinerea*: the cause of grey mould disease. Wiley Online Library. https://doi.org/10.1111/j.1364-3703.2007.00417.x

Wisecaver, J. H., Borowsky, A. T., Tzin, V., Jander, G., Kliebenstein, D. J., Rokas, A. 2017. A Global Coexpression Network Approach for Connecting Genes to Specialized Metabolic Pathways in Plants. *The Plant Cell*, vol. 29, no. 5, pp. 944–959., doi:10.1105/tpc.17.00009.

Wu, W., Wu, Y., Gao, Y., Li, M., Yin, H., Lv, M., Zhao, J., Li, J. and He, K. 2015. Somatic embryogenesis receptor-like kinase 5 in the ecotype Landsberg *erecta* of *Arabidopsis* is a functional RD LRR-RLK in regulating brassinosteroid signaling and cell death control. *Frontier in Plant Sicence* 6:852.

Yamada, K., Yamashita-Yamada, M., Hirase, T., Fujiwara, T., Tsuda, K., Hiruma, K., and Saijo, Y. 2015. Danger peptide receptor signaling in plants ensures basal immunity upon pathogen-induced depletion of BAK1. *The EMBO Journal* 35, 46–6. DOI 10.15252/embj.201591807

Yamaguchi, Y. & Huffaker, A. 2011. Endogenous peptide elicitors in higher plants. *Current Opinion in Plant Biology* 14, 351–357. DOI 10.1016/j.pbi.2011.05.001.

Yamaguchi, Y., Huffaker, A., Bryan, A. C., Tax, E. F. and Ryan, C. A. 2010. PEPR2 is a second receptor for the Pep1 and Pep2 peptides and contributes to defense responses in *Arabidopsis*. *Plant Cell.* 22(2):508-22. doi: 10.1105/tpc.109.068874.

Yamaguchi, Y., Pearce, G. and Ryan, C. A. 2006. The cell surface leucine-rich repeat receptor for AtPep1, an endogenous peptide elicitor in *Arabidopsis*, is functional in transgenic tobacco cells. *Proceedings of the National Academy of Sciences* 103, 10104–10109.

Zhang, H., Huang, L., Dai, Y., Liu, S., Hong, Y., Tian, L., Huang, L., Cao, Z., Li, Dayong. and Song, F. 2015. *Arabidopsis* AtERF15 positively regulates immunity against *Pseudomonas syringae* pv. *tomato* DC3000 and *Botrytis cinerea. Front Plant Sci.* 6:686. doi: 10.3389/fpls.2015.00686

Zhou, L., Lan, W., Jiang, Y., Fang, W., and Luan, S. 2014. A Calcium-Dependent Protein Kinase Interacts with and Activates A Calcium Channel to Regulate Pollen Tube Growth. *Molecular Plant* 7 (2): 369–376. https://doi.org/10.1093/mp/sst125

Zipfel, C., Robatzek, S., Navarro, L., Oakeley, E. J., Jones, J. D., Felix, G. and Boller, T. 2004. Bacterial disease resistance in Arabidopsis through flagellin perception. *Nature* 428*:*764–76.

Zou, J-J., Wei, F-J., Wang, C., Wu, J-J., Ratnasekera, D., Liu, W-X. and Wu, W-H. 2010. Arabidopsis Calcium-Dependent Protein Kinase CPK10 Functions in Abscisic Acid- and Ca2+-Mediated Stomatal Regulation in Response to Drought Stress. *Plant Physiology*, Vol. 154, pp. 1232–1243, www.plantphysiol.org/cgi/doi/10.1104/pp.110.157545